EUROFUSION WPPFC-PR(16) 14826

A Weckmann et al.

Global studies of fuel retention and high-Z metal deposition pattern in the TEXTOR tokamak

Preprint of Paper to be submitted for publication in
22nd International Conference on Plasma Surface Interactions
in Controlled Fusion Devices (22nd PSI)

This work has been carried out within the framework of the EUROfusion Consortium and has received funding from the Euratom research and training programme 2014-2018 under grant agreement No 633053. The views and opinions expressed herein do not necessarily reflect those of the European Commission.

Global material migration of molybdenum in the TEXTOR tokamak

A. Weckmann[1]
P. Petersson[1]
A. Kirschner[2]
P. Wienhold[2]
S. Brezinsek[2]
A. Kreter[2]
A. Pospieszczyk[2]
M. Rubel[1]
[1]Fusion Plasma Physics, Royal Institute of Technology (KTH), 100 44 Stockholm, Sweden
[2]Institute for Energy and Climate Research (IEK-4, Plasma Physics), Forschungszentrum Jülich, 52425 Jülich, Germany

Abstract

MoF_6 injection from a localised source into plasma edge in the TEXTOR tokamak was the last experiment before the final shut-down of the TEXTOR machine. During decommissioning all plasma-facing components (PFCs) became available for surface studies. Detailed mapping of Mo deposition was performed in order to determine its global migration. The concentration of Mo on PFC decays exponentially with distance from the source. The decay length is of the order of 0.1 m on the main PFC and 1 m on the receded components. Also the decay lengths modelled with the ERO code are between 0.15 – 1.3 m, depending on the anomalous cross-field diffusion coefficient. The inner bumper limiter is found to be the major repository for Mo. Material balance measurements show that only up to 22% of the injected Mo was detected on all the PFCs thus indicating a large fraction of injected Mo may have been pumped out before being deposited.

Keywords: *Global transport, Material Migration, High-Z metals, TEXTOR, Plasma-facing components, Molybdenum*

1. Introduction

Several fusion devices, such as JET with ITER-Like Wall [1], ASDEX Upgrade [2] and WEST [3], are equipped with metal walls. Also the plasma-facing wall of ITER will be made of metals [4] in order to minimise accumulation of fuel, especially radioactive tritium [5]. High-Z metals, especially tungsten, have been most prominent candidates for fabrication of plasma-facing components (PFCs) due to their high heat resilience, low erosion by physical sputtering and low tritium uptake [6].

Understanding the transport of high-Z elements from PFCs to the rest of the machine is a key point. So-called prompt re-deposition within the first gyro-radius distance has been considered and studied as a process reducing the long range transport of high-Z metals [7,8]. This process would prevent plasma contamination with high-Z impurities and immediately replenish the wall with returning particles, thus minimising gross erosion. Material migration experiments with tracers were launched to determine, which fraction of released high-Z elements undergo prompt re-deposition, and have shown that a minor fraction is deposited locally in local deposition [9,10,11]. This is because re-deposited metal is effectively re-eroded and it is transported in multi-step process [10,12]. It is thus clear that the majority migrates on global scale. The point is to determine the overall deposition pattern. This possibility was offered with the final shut-down of TEXTOR. The last activity before the machine decommissioning was a marker experiment with locally injected volatile compound of molybdenum: its hexafluoride, MoF_6. It was chosen as a suitable tracer for the prominent PFC candidate W, because a high W background in the vessel was expected from previous experiments. Following the experiment a large number of PFC were retrieved for ex-situ analyses. Local deposition results have been published in [13].

The aim of this contribution is to present a global Mo deposition pattern and to model results with the Monte Carlo transport code ERO [14] in order to obtain a simplified model before moving to a full scale 3D simulation. Details of ERO modelling for Mo transport are addressed in [15].

2. Experimental

TEXTOR was a medium-size limiter tokamak with carbon PFCs and Inconel 625 liner routinely heated up to 250°C for outgassing [16, 17]. MoF_6 was injected locally through a test limiter [18] during the flat top of 31 discharges. A scheme of the experimental set-up and arrays of studied components is shown in Fig. 1. The test limiter was covered with a carbon plate for local deposition analysis; its tip was 1.5 cm outside the last closed flux surface

(LCFS). MoI line emission (388 nm) was recorded with the viewing system described in [19] and used for calculating the injected amount via so called "S/XB values" [20], yielding $5.7 \cdot 10^{20}$ injected Mo atoms. This value was cross-checked and confirmed by pressure drop measurements in the gas injection system.

In the decommissioning 136 limiter tiles were removed; they are listed in Table 1.These were components of the Advanced Limiter Test II (ALTII) limiter which was the main PFC [21], poloidal limiters installed at top and bottom at one toroidal position [16] and the inner bumper limiter which also acted as a shield of dynamic ergodic divertor (DED) [17]. It was the first comprehensive study of this bumper limiter in TEXTOR. In addition, a number of tiles from earlier campaigns were analysed for comparison. Surface studies were carried out with ion beam analysis techniques of different information depth to map and quantify the deposition: Rutherford Backscattering Spectroscopy (RBS) with a 2 MeV ^{4}He beam and Elastic Recoil Detection Analysis (ERDA) using a beam of 36 MeV $^{127}I^{8+}$ ions.

Simplified global modelling of the injected Mo atoms has been done with ERO [14,15] to study the resulting deposition on wall components like the ALT limiter of TEXTOR. Figure 2 presents the set-up of these simulations showing a limiter surface with grazing (0.01°) magnetic field of 2.25 T and the source of Mo particles 3 m away in toroidal direction from the limiter surface. The Mo particles are injected as Mo^{5+} ions with energy of 30 eV. Injection is done into the direction of the limiter at a radial distance of 3 cm away from the limiter surface. In the simulation, edge plasma parameters at the limiter surface in the calculations reflected typical conditions for discharges in TEXTOR heated with neutral beams: electron temperature (T_e) of 30 eV and density (n_e) of $5 \cdot 10^{12}$ cm^{-3} with an exponential decay length of 40 mm in the radial direction. The plasma background flow velocity is assumed to be $v_{Flow} = 1 \cdot 10^4$ m/s along the magnetic field lines in toroidal direction, which has to be compared with the sound velocity of about $5 \cdot 10^4$ m/s under the plasma parameters assumed. The size of the simulation volume is 10 m in toroidal and 5 cm in radial direction. The 1,000,000 injected test particles are traced until they are deposited on the limiter surface or leave the simulation volume.

3. Results and discussion

For this tracer experiment, the quantification of Mo on different PFCs is a key issue. Therefore,two steps had to be performed: (i) subtraction of Mo originating from previous experiments and the liner – Mo was part of the Inconel liner alloy with 4.7 at% [22]; (ii) combining the information of both RBS and ERDA in order to overcome disadvantages of

one method by advantages of the other. The first point was addressed by evaluating tiles removed from TEXTOR before the MoF_6 experiment: Mo background level resulting from earlier experiments and the contribution from the liner erosion was estimated to be $0.8 \cdot 10^{15}$ cm^{-2} on the ALTII limiter and $0{,}6 \cdot 10^{15}$ cm^{-2} on the bumper limiter, on average. This is comparable to Mo concentration levels found on exposed tiles located further away from the injection. The second point was addressed by comparing RBS and ERDA results assuming a co-deposit growth rate of 1-3 nm/s determined in TEXTOR [23, 24], which yields good agreement.

3.1 Material balance

The overall quantities of Mo found on different PFCs are listed in Table 2. On the ALT tiles 2% of the injected amount within the first 200 nm is determined with RBS (with a growth rate of 1-3 nm/s: 4-5%), while with ERDA 4% is determined within the first 500 nm. The correlation between RBS and ERDA for surface Mo is very good: PPMCC = 0.99. Hence RBS and ERDA are in good agreement. The bumper limiter of TEXTOR situated at r=49 cm, i.e. 3 cm behind the LCFS [17], was thus not in direct contact with the plasma. From results of previous WF_6 migration experiments, the bumper limiter has been suspected to be a repository for impurity species [11]. In fact, visual inspection revealed deposits which range from dim grey to shiny colourful appearance. Data for the first 200 nm, i.e. up to a depth accessible for two methods agree well and PPMCC=0.95. Extrapolating RBS results to higher depths – by assuming 1-3 nm/s deposition growth rates and a constant Mo concentration below the first 200 nm – one obtains 6-11%. ERDA measurements suggest as well ca. 11%, hence again we obtain good agreement between the two methods. Absolute uncertainties are ±1.2% to ±2.2%. Analysis performed locally at the point of injection, i.e. the LL1, yielded 6% ±1% of the injected Mo amount. Details about the analysis have been published in [13].

Other places of deposition have also been taken into account, e.g. the poloidal limiter and the sides of ALTII tiles close to the LL1. Roughly 1% of injected Mo is an upper estimate for the poloidal limiter (both top and bottom). For the sides of ALTII tiles next to the MoF_6 injection only negligible amounts of Mo were identified. The same holds for the collector probe operated during the experiment.

In summary, only relatively small fraction of the injected Mo could be found on the PFCs, namely up to 22%. Preliminary examination of liner pieces reveal minute Mo amounts in deposited layers on the liner. However, as deposition rates on the TEXTOR liner were usually

low [25], no large contribution from the liner is to be expected in the Mo balance. Therefore, as inferred from Table 2, the majority of Mo is deposited globally. The ratio of local to global deposition efficiency is about 0.3-0.35. On the global scale, the areal Mo concentrations deposited on ALT and bumper limiter are very similar. Lower Mo amount on the main limiter can be explained by its smaller surface area and erosion of the re-deposited material: The ALT limiter has only 0.4 of the bumper limiter area. Also, the fraction of Mo deposited on ALT limiter vs bumper limiter is ca. 0.4, assuming respectively 4% and 11%.

One concludes that a substantial part of injected Mo is lost and the balance could not be closed. One may suggest that the majority of Mo was lost via the pumps, although certainly not in the form of MoF_6. Another possibility is the deposition of Mo on the liner close to the gas inlet; investigation of liner pieces from this area is ongoing. Closing the Mo balance is not possible without analysis of the entire pumping system and eventually the liner. This may also be the case in other global migration experiments that strive for material balance, as shown for instance in [26].

3.2 Global deposition pattern and modelling

The global pattern of Mo is based on the RBS results and represents the Mo distribution in the top 50-100 nm thick layer, i.e. at the very surface, see Fig. 3 (all PFC surfaces projected into one plane). The pattern was obtained by interpolating over 570 RBS measurement points with a linear radial basis function approach. It represents the averaged distribution. Some deviations are caused by highly localised deposition and re-erosion effects.

On the PFCs, exponential decay of impurity concentration could be found in the interpolated curves. These curves fit the values further away from LL1 on ALT and bumper limiter, but have poorer match close to LL1, due to high concentration variations on short length scales. The decay lengths mentioned hereafter are thus for description of global deposition, but not close to an impurity source. Uncertainties given for decay lengths do not account for local concentration variation.

The global deposition pattern of Mo has several characteristic features. It is mostly influenced by the MoF_6 injection (LL1). Mo is deposited close to the point of injection, within about ±15° toroidally. Outside this region, Mo concentration is close to the background levels. The Mo concentration falls off exponentially on ALT and bumper limiter. Decay lengths in poloidal and toroidal direction can be found in Table 3. Deposition takes place predominantly

in co-direction on the ALT limiter. After background subtraction, Mo concentration on ALT limiter is on average $0.7 \cdot 10^{15}$ cm^{-2} with maximum $4.8 \cdot 10^{15}$ cm^{-2} close to the injection. On the bumper limiter it is on average $0.7 \cdot 10^{15}$ cm^{-2} with maximum $4.7 \cdot 10^{15}$ cm^{-2}. At the top of the bumper limiter (Fig. 3, coordinates [+20; -240]), a high Mo concentration was detected although this region is poloidally 150° away from the injection. On the first ALT blade in counter direction (Fig. 3, coordinates [-20; -45]), the Mo content is increased locally without a connection to the injection area. Additionally, visual inspection of two tiles from that area showed flaky metallic deposits. It is likely not resulting from the MoF_6 injection but rather from metallic debris. On the collector probe, the exponential decay of Mo concentration along radial direction was detected 4 cm away from the LCFS, with decay lengths of 1.1 cm in co-direction and 2.9 cm in the counter-direction.

For the simulations two different values have been assumed for the anomalous cross-field diffusion coefficient D_{perp} of the Mo^{5+} ions, namely 0.02 and 0.2 m^2/s. The value of 0.2 m^2/s is within the range of typical assumptions and observations for D_{perp} in the edge plasma of tokamaks, see e.g. [42, 43]. The smaller value has been used to study the influence of the cross field diffusion on the Mo deposition.

Figure 4 shows the resulting Mo deposition on the limiter surface; the profile for D_{perp}=0.02 m^2/s has been multiplied with 9 to improve its visibility. After reaching a maximum at a certain toroidal location at the limiter surface, the Mo deposition decreases exponentially with a decay length of about 130 cm for D_{perp} =0.02 m^2/s. In the case of D_{perp} = 0.2 m^2/s the steep decay after the maximum can also be described with an exponential function but with much smaller decay length of about 15 cm. The modelled increase of the deposition at the beginning of the limiter surface will disappear in both cases if the source of the injection is moved farther away from the limiter surface. The relative amount of deposited Mo particles is about 60% for D_{perp}=0.02 m^2/s and 84% for D_{perp}=0.2 m^2/s. Please note that no re-erosion of once deposited Mo is included in the simulation. Particles not deposited on the limiter surface leave the simulation volume in maximum toroidal and minimum radial direction, in case of the larger diffusion coefficient also in maximum radial direction.

In summary, the exponential decay is in accordance with previous findings [15, 44] and with ERO simulations with the peak close to the point of origin. ERO simulations yield decay lengths of the same order as in the experiment. For D_{perp} = 0.2 m^2/s the simulated decay length agrees well with the experimental one of Mo: 15 cm versus 12±5 cm.

3.3 Role of flows

In the discussion of the deposition patterns of Mo poloidal and toroidal flows in the TEXTOR machine are to be taken into account. This is apparent by the locations of concentration maxima on the PFCs. One has to compare the toroidal and poloidal positions of deposition maxima with respect to the sources of impurities. The goal is to understand the impact of flows on global transport and deposition. The toroidal shift observed for Mo deposition maxima on both limiter (ALTII and bumper limiter) bottoms is around 5° or ca. 15 cm, see Fig. 3. The poloidal distance from the injection point at LL1 is 25 cm towards both limiters. Hence, at the bottom of TEXTOR the ratio of poloidal to toroidal flow velocity would have been ca. ±1.7, and equal in either direction: towards both the ALTII and bumper limiter bottoms.

In summary, the data suggests that flows have the main role in determining the area of first deposition. They furthermore heavily influence global patterns and final deposition: E.g., as a consequence of poloidal flows towards the bumper limiter, all investigated high-Z impurities were deposited on top and bottom of the bumper limiter. The equator region exhibits a lower material concentration. The observation of flows towards the bumper limiter from both top and bottom, together with enhanced deposition of fuel and other impurity species emphasises its role as the major repository in TEXTOR.

4 Concluding remarks

For the first time-ever such comprehensive studies of PFC combined with modelling have been performed to obtain a global deposition pattern of high-Z metals. A strong point is that this work takes carefully into account both the last well defined gas injection (localised source) experiment and earlier operation history. The area of first deposition is determined by flows. Subsequent re-erosion and prompt re-deposition yields exponential decay with decay lengths of the order of 0.1-1 m, depending on PFC, element mass and residual time in the machine. ERO modelling predicts exponential decay along toroidal direction, as seen in the actual pattern. Decay lengths in simulation and experiment agree well. It encourages further modelling efforts to extend work to full scale 3D geometry. For this one has to know a global qualitative and quantitative picture of deposition: map and quantities. This time measurements have been extended to a large number of tiles of the inner bumper limiter showing the importance of plasma-facing recessed areas acting as repository not only for high-Z elements but also for fuel species. It should be stressed once again that even such broad analysis activity has resulted in the identification of only limited amount of tracer species: up to 22%. This is not a result specific just for TEXTOR, but a feature known from many other marker

experiments in the past [26, 27]. The answer would most probably come from studying the entire pumping system and liner, what – unfortunately – is not technically feasible.

Acknowledgements

This work has been carried out within the framework of the EUROfusion Consortium and has received funding from the Euratom research and training programme 2014-2018 under grant agreement No 633053. The views and opinions expressed herein do not necessarily reflect those of the European Commission. The work has been partly funded by the Swedish Research Council (VR) through contracts no. 621-2012-4148 and 2015-04844. The Ion Technology Centre, Uppsala University, Sweden provided all ion beam analysis equipment and is therefore highly acknowledged. We would like to thank Antti Hakola for very helpful suggestions, Petter Ström for help in PFC analysis, Michael Rack for collector probe operation, Jan W. Coenen for spectroscopic data and helpful discussion, Oskar Eliasson and Pavel Kupsc for the probe analysis and Jury Romazanov for helpful comments on interpolation.

Bibliography

[1] G. F. Matthews et al, JET ITER-like wall – overview and experimental programme, Phys. Scr. T145 (2011).

[2] R. Neu et al., Overview on plasma operation with a full tungsten wall in ASDEX Upgrade, J. Nucl. Mater. 438 (2013) 34-41.

[3] C. Bourdelle et al., WEST Physics Basis, Nucl. Fusion. 55 (2015).

[4] ITER Organisation, The ITER tokamak. http://www.iter.org/mach, 2016 (accessed March 2016).

[5] J. Roth et al., Recent analysis of key plasma wall interaction issues for ITER, J. Nucl. Mater. 390-391 (2009) 1-9.

[6] V. Philipps, Tungsten as material for plasma-facing components in fusion devices, J. Nucl. Mater. 415 (2011) S2-S9.

[7] D. Naujoks and R. Behrisch, Erosion and redeposition at the vessel walls in fusion devices, J. Nucl. Mater. 220-222 (1995) 227-230.

[8] D. Naujoks et al., Tungsten as target material in fusion devices, Nucl. Fusion. 36 (1996) 671-687.

[9] M. Rubel et al., Tracer techniques for the assessment of material migration and surface modification of plasma-facing components, J. Nucl. Mater. 463 (2015) 280-284.

[10] W. R. Wampler et al., Measurements of net erosion and redeposition of molybdenum in DIII-D, J. Nucl. Mater. 438 (2013) 822-826.

[11] M. Rubel et al., Tungsten migration studies by controlled injection of volatile compounds, J. Nucl. Mater. 438 (2013) 170-174.

[12] S. Brezinsek et al., Quantification of tungsten sputtering at W/C twin limiters in TEXTOR with the aid of local WF6 injection, Phys. Scr. T145 (2011).

[13] A. Weckmann et al., Local migration studies of high-Z metals in the TEXTOR tokamak, Phys. Scr. T167 (2015) 014058.

[14] A. Kirschner et al., Simulation of the plasma-wall interaction in a tokamak with the Monte Carlo code ERO-TEXTOR, Nucl. Fusion 40 (2000) 989-1001.

[15] A. Kirschner et al. This conference.

[16] O. Neubauer et al., Design features of the tokamak TEXTOR, Fusion Sci. Technol. 47 (2005) 76-86.

[17] B. Giesen et al, Technical lay-out of the dynamic ergodic divertor, Fusion Eng. Des. 37 (1997) 341-346.

[18] A. Kreter et al., Study of local carbon transport on graphite, tungsten and molybdenum test limiters in TEXTOR by (CH4)-C-13 tracer injection, J. Nucl. Mater. 363 (2007) 179-183.

[19] S. Brezinsek et al., Characterization of deuterium recycling flux in front of a graphite surface in the TEXTOR tokamak, Plasma Phys. Contr. F. 47 (2005) 615-634.

[20] A. Pospieszczyk et al., Determination of rate coefficients for fusion-relevant atoms and molecules by modelling and measurement in the boundary layer of TEXTOR, J. Phys. B – At. Mol. Opt. 43 (2010).

[21] R. W. Conn et al., The toroidal belt pump limiter, ALT-II, in the TEXTOR tokamak, Fusion Eng. Des. 13 (1990) 251-259.

[22] Special Metals Corporation, Inconel 625 datasheet. http://www.specialmetals.com/documents/Inconel%20alloy%20625.pdf, August 2013 (accessed: April 2016).

[23] M. Mayer et al., Hydrogen inventories in nuclear fusion devices, J. Nucl. Mater. 290-293 (2001) 381-388.

[24] M. Rubel, P. Wienhold, D. Hildebrandt, Fuel accumulation in co-deposited layers on plasma facing components, J. Nucl. Mater. 290-293 (2001) 473-477.

[25] J. v. Seggern et al., Long term behaviour of material erosion and deposition on the vessel wall and remote areas of TEXTOR, J. Nuc. Mat 313-316 (2003) 439-443.

[26] J. Strachan et al., Modelling of carbon migration during JET ^{13}C injection experiments, Nucl. Fusion 48 (2008) 105002.

[27] J.P. Coad et al., Overview of material re-deposition and fuel retention studies at JET with the Gas Box divertor, Nucl. Fusion. 46 (2006) 350.

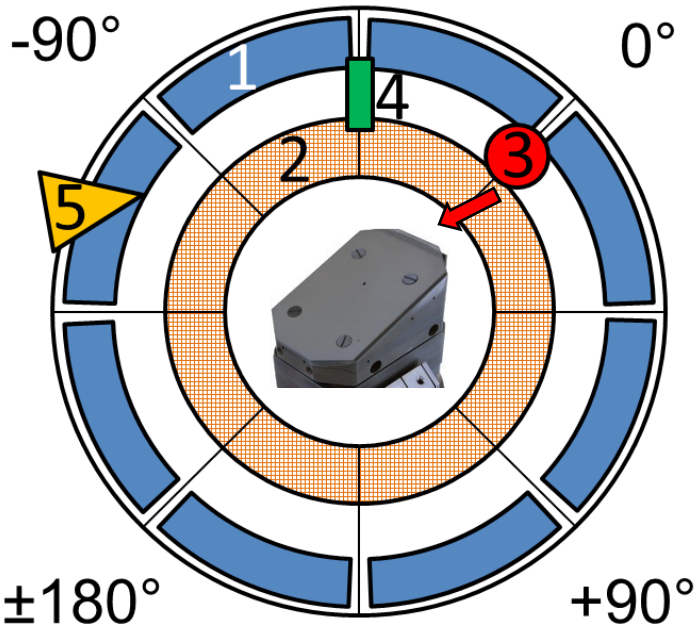

Figure 1 Schematic view on all analysed PFCs and wall probes: (1) ALTII main limiter, (2) bumper limiter, (3) roof-shaped test limiter with gas injection inlet (details: centre), (4) poloidal limiter, (5) collector probe.

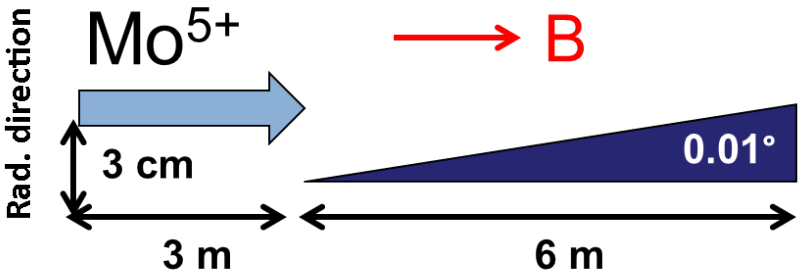

Fig. 2. Geometry in ERO simulation of global deposition.

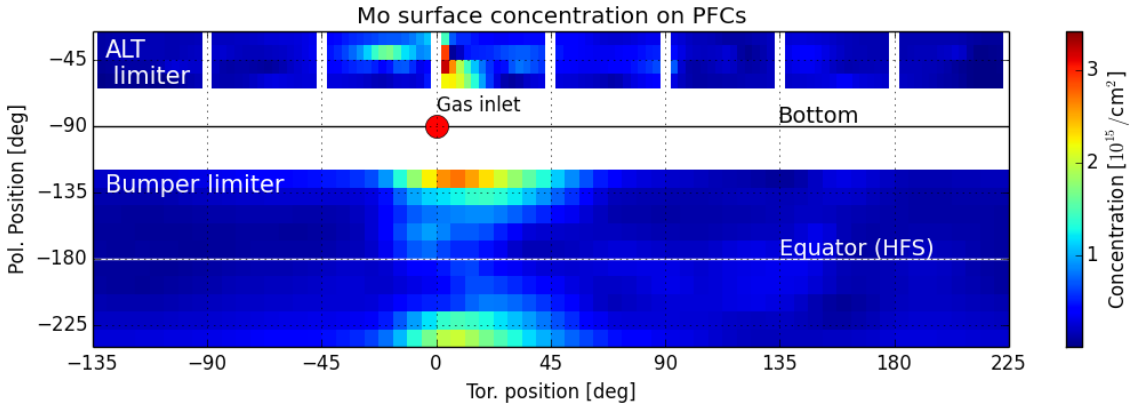

Figure 3: Interpolation of Mo surface concentration measurements with RBS, in 10^{15} cm^{-2}. For visualisation the PFC surfaces have been projected into φ-θ plane, with θ=0 at the low-field side and θ=-180 on the high-field side (HFS).

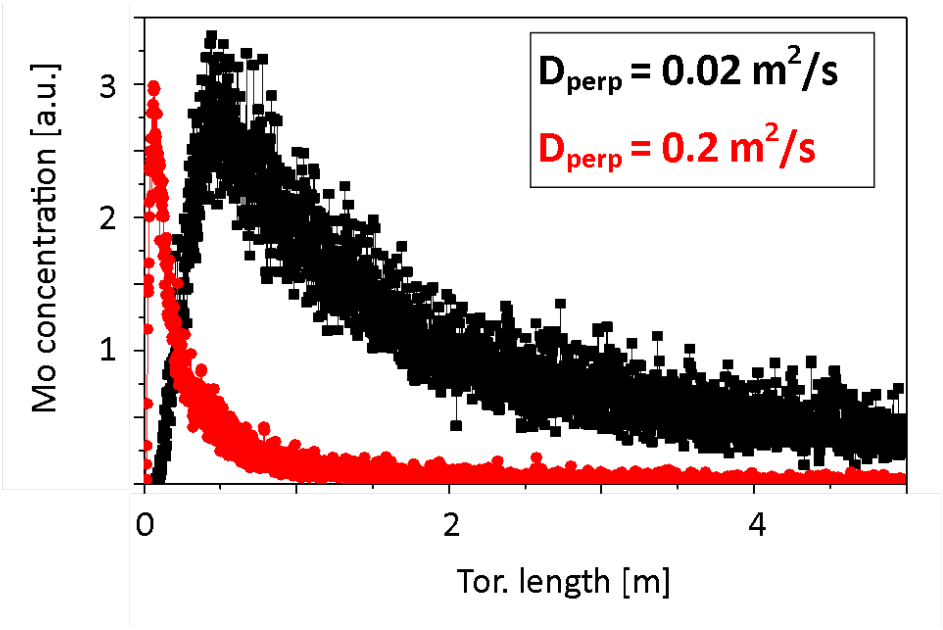

Figure 4: ERO simulation of global deposition, toroidal pattern.

Table 1: Amount of analysed PFCs and liner parts, with means of analysis and purpose.

PFC (all carbon)	No. analysed PFCs
ALT main limiter	37 (exposed) + 3 (unexposed)
Bumper limiter	99 (exposed) + 3 (unexposed)
LL1 cover plate	1 (exposed)
Poloidal limiter	6 (exposed)
Collector probe	1 (exposed)

Table 2: Amount of Mo found on analysed PFCs and LL1, relative to the injected amount of MoF_6, and peak concentration. More details on local Mo deposition and LL1 analysis can be found in [13].

PFC, machine parts	Amount of Mo rel. to injected Mo amount [%]	Max. Mo surface concentration [10^{15}/cm^2]
ALT main limiter	2±0.4 (RBS) – 4±0.8 (ERDA)	4.8
Bumper limiter	6±1.2 (RBS) – 11±2.2 (ERDA)	4.7
LL1 cover plate	6±1 [13]	12 000 (details in [13])
Poloidal limiter	≤ 0.9	5.4
Collector probe	0.02	10.2
LL1 inner channels	≤ 0.1 [18]	38 (beneath cover plate)

Table 3: Exponential decay lengths of global Mo and W patterns in toroidal and poloidal direction, based on linear interpolations.

PFC		Decay length – Mo [cm]	
Toroidal direction		**Co**	**Counter**
ALT limiter		12±5	26±7
Bumper limiter	Top	103±21	66±14
	Bottom	105±21	84±18
Poloidal direction		**Top**	**Bottom**
Bumper limiter		20±4	15±3